

НАЦИОНАЛЬНАЯ АКАДЕМИЯ НАУК БЕЛАРУСИ
ИНСТИТУТ ТЕПЛО- И МАССООБМЕНА им. А. В. ЛЫКОВА
Журнал основан в январе 1958 г.

ІФН



ІНЖЕНЕРНО-ФІЗИЧЕСКИЙ ЖУРНАЛ

JOURNAL
OF ENGINEERING PHYSICS
AND THERMOPHYSICS

Отдельный оттиск
Offprint

Том 91, № 5

Vol. 91, No. 5

СЕНТЯБРЬ–ОКТЯБРЬ
SEPTEMBER–OCTOBER

2018

ИНЖЕНЕРНО-ФИЗИЧЕСКИЙ ЖУРНАЛ

Основан в январе 1958 г.

2018. ТОМ 91, № 5 (СЕНТЯБРЬ–ОКТЯБРЬ)

СОДЕРЖАНИЕ

ТЕПЛО- И МАССОПЕРЕНОС В ДИСПЕРСНЫХ И ПОРИСТЫХ СРЕДАХ

Ларина О. М., Зайченко В. М., Исьемин Р. Л., Михалев А. В., Муратова Н. С., Кузьмин С. Н., Теплицкий Ю. С., Бородуля В. А., Бучилко Э. К. О расчете скорости начала псевдоожижения квазидисперсного зернистого слоя.....	1187
Пицуха Е. А. О численном моделировании гидродинамики и перемешивания газовых потоков в вихревой камере	1193
Хабеев Р. Н., Хабеев Н. С. О собственной частоте свободных колебаний газовой оболочки, окружающей твердую частицу или каплю	1204
Тукмаков А. Л., Тукмаков Д. А. Генерация акустических возмущений движущейся заряженной газовзвесью.....	1207
Губайдуллин Д. А., Федоров Ю. В. Наклонное падение акустической волны на слой пузырьковой жидкости	1214
Коринчук Д. Н., Снежкин Ю. Ф. Моделирование процесса высокотемпературной сушки композиционной смеси в аэродинамической сушилке комплекса производства биотоплива.....	1221
Коляно Я. Ю., Сасс Т. С., Иваник Е. Г. Моделирование кондуктивной сушки полиграфических материалов капиллярно-пористой коллоидной структуры	1231
Шагапов В. Ш., Тазетдинова Ю. А., Гиззатуллина А. А. К проблеме разработки месторождений с высоковязкой нефтью тепловыми методами	1242
Нурисламов О. Р., Лепихин С. А. Особенности разложения гидрата во влажном пористом пласте конечной протяженности при депрессионном воздействии	1250
Кутя Т. В., Мартынюк П. Н. Математическое моделирование увлажнения и расчет коэффициента запаса устойчивости грунта на склоне с учетом влияния тепло- и массопереноса.....	1256

ТЕПЛОПРОВОДНОСТЬ И ТЕПЛООБМЕН В ТЕХНОЛОГИЧЕСКИХ ПРОЦЕССАХ

Ефимов К. Н., Овчинников В. А., Якимов А. С. Влияние вращения конуса, затупленного по сфере, на теплообмен в нем при сверхзвуковом обтекании под углом атаки	1266
Карлович Т. Б. Теплопередача круглых ребристых труб при неравномерном эксплуатационном загрязнении межреберного пространства.....	1278
Мансуров Р. Ш., Федорова Н. Н., Ефимов Д. И., Косова Е. Ю. Математическое моделирование теплотехнических характеристик наружных ограждений с воздушными прослойками.....	1287
Келбалиев Г. И., Расулов С. Р., Илюшин П. Ю., Мустафаева Г. Р. Кристаллизация парафина из нефти и осаждение асфальто-парафинистых веществ на поверхности труб	1294
Уразов Р. Р., Гималтдинов И. К., Ишмуратов Т. А., Хусаинов И. Г. Моделирование работы системы охлаждения возвратного этилена при производстве полиэтилена высокого давления	1300

ТЕПЛО- И МАССОПЕРЕНОС В ПРОЦЕССАХ ГОРЕНИЯ

Базылев Н. Б., Фомин Н. А. Кросс-корреляционный анализ в цифровой спектр-фотографии.....	1308
Антонов Д. В., Волков Р. С., Войтков И. С., Жданова А. О., Кузнецов Г. В. Влияние специализированных добавок и примесей в водном аэрозоле на условия подавления лесного пожара	1318
Крайнов А. Ю., Моисеева К. М. Моделирование искрового зажигания бидисперсной аэровзвеси угольной пыли	1328
Евдокимов О. А., Гурьянов А. И., Пиралишвили Ш. А., Веретенников С. В., Гурьянова М. М. Особенности формирования диффузионных реагирующих струй в закрученном воздушном потоке	1335

НАНОСТРУКТУРЫ

Зарубин В. С., Савельева И. Ю., Сергеева Е. С. Оценки эквивалентных коэффициентов теплопроводности углеродных нанотрубок	1342
Рудяк В. Я., Борд Е. Г. О гидродинамической устойчивости течений Пуазейля и Куэтта наножидкостей в канале между концентрическими цилиндрами.....	1351
Гончаров В. К., Козадаев К. В., Мельников К. А., Микитчук Е. П., Новиков А. Г. Атмосферное лазерное осаждение ГКР-активных коллоидов благородных металлов (Ag, Au, Pt).....	1360
Temirgaliyeva T. S., Nazhipkazy M., Nurgain A., Mansurov Z. A., and Bakenov Zh. B. Synthesis of Carbon Nanotubes on a Shungite Substrate and Their Use for Lithium–Sulfur Batteries	1365

ГИДРОГАЗОДИНАМИКА В ТЕХНОЛОГИЧЕСКИХ ПРОЦЕССАХ

Nath G., Sumeeta Singh, and Pankaj Srivastava. Exact Solution for a Magnetogasdynamical Cylindrical Shock Wave in a Self-Gravitating Rotating Perfect Gas with Radiation Heat Flux and Variable Density	1372
Горский В. В., Ковальский М. Г., Пугач М. А. Новый инженерный метод расчета теплообмена в ламинарно-турбулентном пограничном слое	1383

ПРОЦЕССЫ ПЕРЕНОСА В РЕОЛОГИЧЕСКИХ СРЕДАХ

Славнов Е. В., Скульский О. И., Шакиров Н. В., Судаков А. И., Кузнецова Ю. Л., Кряжевских О. В. Реологическое поведение сверхвысокомолекулярного полиэтилена	1392
Кадыров А. И., Абайдуллин Б. Р., Вачагина Е. К. Исследование затухания закрутки течения обобщенной ньютоновской жидкости	1402

ТЕПЛОФИЗИЧЕСКИЕ СВОЙСТВА

Пилипенко В. А., Солодуха В. А., Горушко В. А. Влияние быстрой термической обработки на электрофизические свойства двуокиси кремния.....	1408
Большев К. Н., Заричняк Ю. П., Иванов В. А. Определение теплопроводности методом начальной стадии разогрева образца постоянным тепловым потоком.....	1413

РАЗНОЕ

Косенко И. А., Денисов А. Е., Данилаев М. П., Пашин Д. М. Эффект генерации Оже-дуплексов.....	1418
---	------

Ответственный за выпуск: Л. Н. Шемет

Подписано в печать 03.09.2018. Формат 60×84½. Бумага офсетная.
Усл. печ. л. 27,55. Уч.-изд. л. 23,25. Тираж 91 экз. Заказ 171.

Отпечатано в Республиканском унитарном предприятии «Издательский дом «Беларуская навука».
Свидетельство о государственной регистрации издателя, изготовителя, распространителя печатных изданий №1/18 от 02.08.2013.
ЛП № 02330/455 от 30.12.2013.

220141, г. Минск, ул. Ф. Скорины, 40

© Институт тепло- и массообмена им. А. В. Лыкова Национальной академии наук Беларуси

UDC 544.018.2

T. S. Temirgaliyeva^{1,2}, M. Nazhipkazy^{1,2}, A. Nurgain², Z. A. Mansurov^{1,2}, and Zh. B. Bakenov³

**SYNTHESIS OF CARBON NANOTUBES ON A SHUNGITE SUBSTRATE
AND THEIR USE FOR LITHIUM-SULFUR BATTERIES**

A shungite mineral has been used as a support material of catalyst particles to synthesize multiwalled carbon nanotubes (MWCNTs). Raman spectroscopy enabled us to follow the formation of MWCNTs. The morphology of synthesized MWCNTs was investigated by a scanning electron microscope and a transmission electron microscope. As a result of simple heat treatment at 300°C for 3 h in an inert atmosphere, a novel sulfur/multiwalled carbon nanotubes/polyacrylonitrile (S/MWCNT/PAN) composite was synthesized. These methods of obtaining MWCNTs and S/MWCNT/PAN composite based on heat treatment possess the advantages of simplicity and low cost. The introduction of MWCNTs into the composite gives a highly conductive and mechanically flexible framework with an enhanced electronic conductivity and the ability to absorb polysulfides between the Li anode and cathode, which leads to an enhanced cyclability and a higher coulombic efficiency. The cell with this S/MWCNT/PAN ternary composite cathode demonstrates a stable reversible specific discharge capacity of 800 mA · h · g⁻¹ after 50 cycles at a battery C-rate of 0.2 C.

Keywords: *multiwalled carbon nanotubes, lithium-sulfur batteries, composite, CVD.*

Introduction. Carbon nanotubes (CNTs) have unique electronic properties which can be used to make nanoelectronic devices, such as transistors and lithium-ion batteries, with excellent field emission properties, such as a low emission threshold, high emission current density, and high stability. CNTs can be expected to exhibit the excellent strength, resistance, elastic, and isotropic properties [1]. These properties indicate that CNTs can have broad application prospects in numerous areas. Among several techniques of CNTs synthesis available today, chemical vapor deposition (CVD) is the most popular and widely used because of its low setup cost, high production yield, and easiness of scale-up. In this connection, this paper considers the mechanism of the growth and mass production of CNTs by CVD. In [2] it is shown that the catalyst and reaction temperatures are important factors which affect the yield of CNTs.

Many efforts have been made for sulfur impregnation of various carbon matrixes, such as mesoporous carbons, carbon fiber, carbon nanotubes, and graphene. Although sulfur is considered to be one of the promising candidates for the next generation of lithium-ion and lithium/sulfur (Li/S) batteries because of its high specific capacity (1672 mA · h/g) and an extremely low cost of 150 USD/t (at 40 USD/kg for LiCoO₂), there are several challenging problems in realizing Li/S batteries. First, elemental sulfur is a very insulating material, and sulfur-based cathodes require a large amount of conducting additives (usually more than 50 wt.%), such as conducting polymer (e.g., polypyrrole (PPY) [3], cyclized polyacrylonitrile (PAN) [4], etc.) and conducting carbon materials (e.g., acetylene black, carbon nanotubes, graphene, etc.).

Second, lithium polysulfides, i.e., reduced forms of sulfur, dissolve into an electrolyte solution, resulting in a capacity decrease; therefore, the stabilization of polysulfides is necessary. So far, S/PAN composites show relatively stable cycle life performance, even in LiPF₆/carbonate-based electrolyte solutions: it has been explained that the nanoscopic (or subnanoscopic) presence of sulfur/polysulfides in cyclized PAN contributes to the polysulfide stabilization. The S/PAN binary composites or S/PAN/conducting carbon ternary composites were first suggested by Wang et al. [5].

¹ Al-Farabi Kazakh National University, Kazakhstan, 050040, Almaty, al-Farabi Ave., 71; ²Institute of Combustion Problems, Kazakhstan, 050012, Almaty, Bogenbai Batyr Str., 172; ³Nazarbayev University, National Laboratory, Kazakhstan, 010000, Astana, Kabanbay Batyr Ave., 53; email: tolganay.01@mail.ru. Original article submitted January 31, 2017.

In the specific case of a Li/S cell, CNTs have at least four specific features that justify interest in them: i) CNTs have a high surface area and a large surface to volume ratio. These materials can therefore be thought to provide an ideal interconnected conductive scaffold to locate sulfur and its poorly conductive reduction products in the cathode; ii) the CNTs microstructure may also be beneficial for kinetic trapping long-chain lithium polysulfides (LiPS) in the cathode, which, without compromising an interfacial contact between active materials and electrolyte, limits their dissolution and release into the electrolyte; iii) at the CNTs concentrations above the percolation threshold, they create a mechanically strong scaffold in the cathode. The integration of a polymer binder and sulfur creates a mechanically robust electrode which is able to accommodate periodic volume expansion and contraction of sulfur that accompany its redox reaction with lithium; iv) with worldwide efforts focused on economical processes for large-scale and cost-effective manufacture of CNTs, a variety of CNTs is now available at modest prices of 0.10–25 USD/g. It is predicted that this cost could drop to as little as 10–30 USD/kg within the next ten years when the production capacity is expected to reach hundreds of thousands tons annually [6].

In this work, we pioneered the use of a shungite mineral (Taldykorgan, "Koksu") as a support material of a catalyst for synthesis of multiwalled carbon nanotubes. Synthesized nanotubes were used as a composite material for Li/S batteries. The resulting composite cathode demonstrated excellent electrochemical performance.

Experimental. *Material preparation.* Carbon nanotubes were grown by one-step CVD at the ambient pressure. Figure 1 gives a brief illustration of our thermal catalytic CVD system. This system is based on a modified Lindberg/BlueM furnace and consists of a quartz reaction tube with an inner diameter of 35 mm and a length of 450 cm. The central part of the reactor (where the sample is kept) can maintain a stable temperature up to 1000°C. The temperature was measured by a chromel–alumel thermocouple. The growth process was performed via the catalytic decomposition of a propane–butane gas mixture on a shungite substrate with a previously prepared catalyst.

A high-purity propane–butane gas mixture was selected as a carbon source and a high-purity Ar, as an inert gas. Nickel salt has obvious catalytic effect, so that nickel nitrate was chosen as a catalyst for the CNTs preparation. Shungite with nickel nitrate were heated to 400–500°C for optimizing the catalyst particles.

A typical growth procedure involves an initial preheating step in an argon atmosphere (80 ml/min). The propane–butane gas mixture was then introduced into the gas stream for 30 min at a fixed flow rate of 80–100 mL/min. The growth temperature was set at a fixed value for a given process (e.g., 800°C). The procedure was completed with the cooling step in an inert atmosphere. In general, the synthesis was performed over a wide range of temperatures from 650 to 800°C at atmospheric pressure. Figure 2 shows the catalyst in a porcelain boat before and after the use of the CVD method of synthesis of carbon nanotubes.

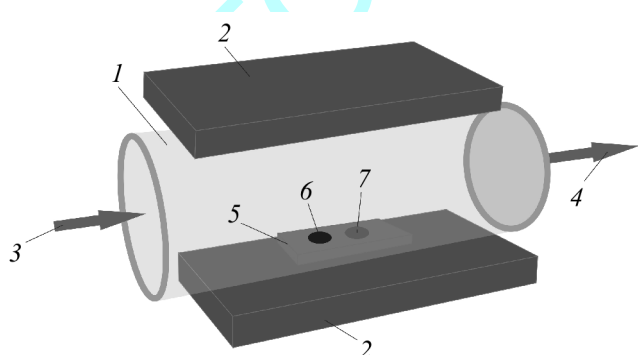


Fig. 1. Schematic of the catalytic CVD setup using a propane–butane mixture as a carbon feeding gas: 1) quartz tube; 2) furnace; 3) gas inlet; 4) gas outlet; 5) porcelain boat; 6) CNTs; 7) catalysts.

Material characterization. The crystalline phases of the composite were determined by X-ray diffraction (XRD, D8 Discover; Bruker) with CuK α radiation. A scanning electron microscope (SEM) (Quanta 3D 200i Dualsystem, FEI) was used to examine the orientation and length of CNTs produced. A micro-Raman spectrometer NTegra Spectra (NT-MDT, Russia) was employed to structurally characterize the CNTs. A high-resolution transmission electron microscope (HRTEM) (JEOL JEM-2100) was used to image the morphology and structure of the material grown. To determine the carbon content, the TGA analysis (SDT Q600) of the sample was conducted.



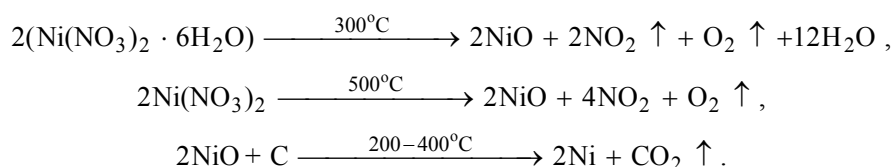
Fig. 2. Catalyst before (a) and after the CVD method use (b).

Electrochemical measurements. The S/MWCNT/PAN composite was prepared by mixing 80% S, 1% MWCNTs, and 19% PAN. Then all materials were grounded in a mortar and heat-treated at 300°C for 3 h in a tube furnace in argon to form a molecular-level composite. After heat treatment, the samples were weighted, and the percentage of S was calculated to be equal to 42%. Then the composite cathode was prepared by mixing 80 wt.% S/MWCNT/PAN composite, 10 wt.% polyvinylidene fluoride (PVDF) (Kynar, HSV900) as a binder, and 10 wt.% acetylene black (MTI, 99.5% purity) conducting agent in 1-methyl-2-pyrrolidinone (NMP, Sigma-Aldrich, ≥99.5% purity). The resultant slurry was spread uniformly on a carbon-coated aluminum foil, using a doctor blade, and dried at 70°C in a vacuum oven for 24 h. The resulting cathode film was used to prepare cathodes by punching circular disks 15 mm in diameter. The electrochemical performance of the S/MWCNT/PAN composite cathode was investigated, using coin type cells (CR2032) assembled in an argon-filled glovebox (MasterLab, MBraun), with lithium metal discs as an anode, porous polypropylene membrane as a separator (Celgard 2400), and a 1M lithium bis(trifluoromethanesulfonyl)imide (LiTFSI) as a liquid electrolyte. The electrodes were pressed in order to decrease the thickness and thereby to achieve a good contact between the active materials. The assembled coin cells were tested galvanostatically on a multichannel battery tester (Neware) versus the standard electrode potential of Li⁺/Li. The applied currents and specific capacities were calculated on the basis of the weight *W* of S in each cathode. All electrochemical measurements were performed at room temperature.

Results and Discussion. The results of X-ray diffraction of the shungite used as a support material for catalyst particles in CNTs growth before the CVD process are shown in Fig. 3. The elemental composition of the shungite is presented in Table 1. It can be seen from the X-ray diffraction data that the shungite contains metals, such as Fe, Cr, Ca, Ni, Cu, K, Ti, Si, Mn, V, Zn, and Al. For CNTs synthesis, hydrogen is usually used as a reducing agent, but in our case, a reducing agent is the carbon contained in the shungite [7].

The morphology of the shungite before the CVD process which is obtained by scanning electron microscopy is shown in Fig. 4. From the SEM image of the shungite it is seen that the mineral is composed of dispersed particles with diameters ranging from 1 to 20 μm.

The main tool for optimizing catalytic active sites of the nickel catalyst at the shungite substrate, which was used as a catalyst for growing CNTs, is the nickel reduction at 400–500°C. At these temperatures, the reaction of decomposition of nickel nitrate followed by the reduction to nickel particles takes place as follows:



It is seen from this reaction that the catalyst particles of nickel, which will contribute to CNTs growth on the shungite substrate, were formed.

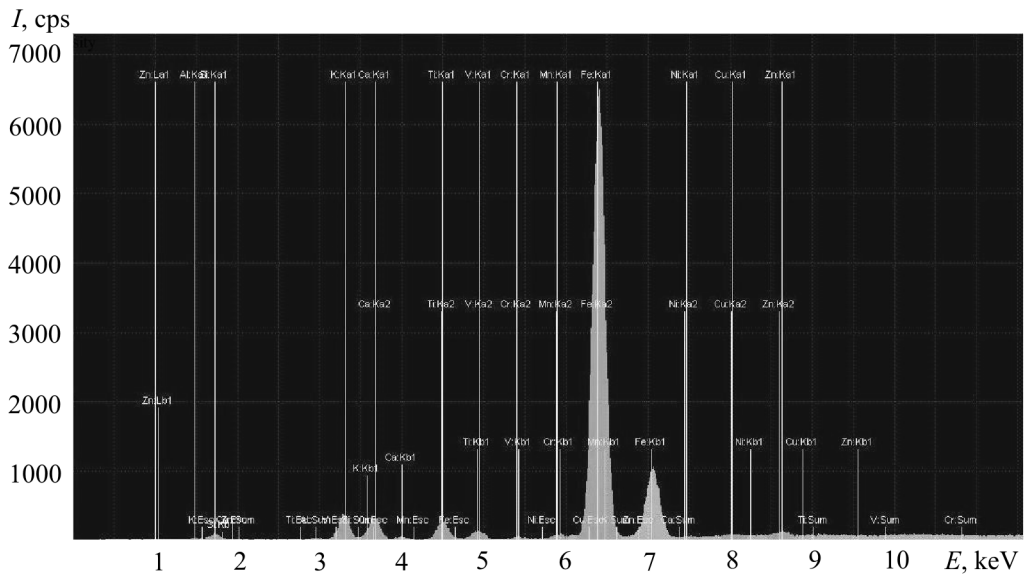


Fig. 3. X-ray diffraction pattern of the shungite.

TABLE 1. Elemental Composition of Shungite

Element	c , %	I , a.u.
Fe	23.659	587.72
Cr	0.079	2.59
Ca	2.816	21.11
Ni	0.041	0.71
Cu	0.127	2.37
K	8.127	23.45
Ti	1.341	18.14
Si	50.816	5.25
Mn	0.127	2.92
V	0.342	8.89
Zn	0.269	5.26
Al	12.256	0.40

The Raman spectral evolution of the sample obtained after the CVD process at 800°C by pyrolysis of a propane–butane gas mixture is seen in Fig. 5. This figure shows three typical Raman spectra of nanotubes obtained under the above growth conditions. The spectra contain three common Raman bands which are more typical for MWCNTs. The G band has a shoulder at 1555 cm^{-1} , which is indicative of metallic CNTs. The D band has a very high intensity, which points to the higher defectiveness of the carbon material. The I_D/I_G ratio is equal to unity, which suggests increased formation of disordered carbon material and a higher surface area of multiwalled carbon nanotubes. This led to an increase in the specific capacity of the carbon nanotubes grown by one-step CVD at 800°C.

The surface morphology and structure of the MWCNTs imaged by TEM and SEM are presented in Fig. 6. It shows the formation of MWCNTs on the shungite surface in the presence of Ni particles. It can also be seen that MWCNTs stack irregularly, forming a highly porous structure. This porous MWCNTs network could serve not only as a current collector for long-range electron transfer, but also as a macroporous robust matrix to aid in electrolyte penetration and to prevent sulfur particles segregation [8]. It should be noted that the decomposition of propane at higher temperatures leads to the deposition of additional carbonaceous compounds besides nanotubes. These compounds are barely visible in Fig. 6b.

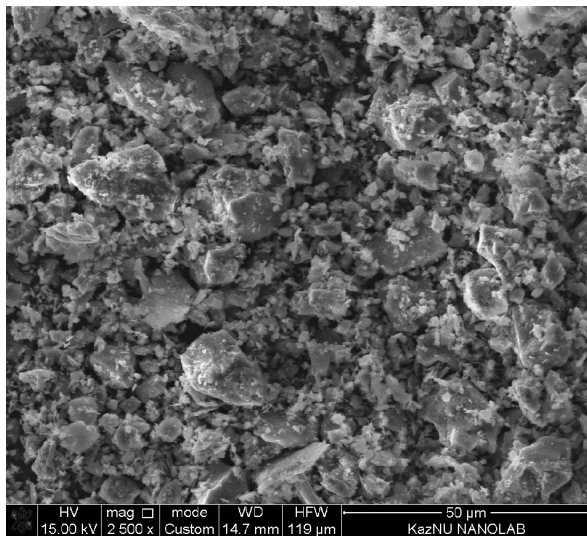


Fig. 4. SEM image of the shungite.

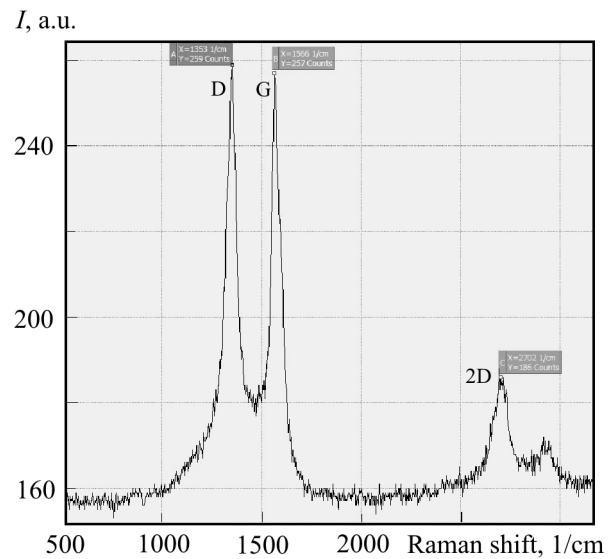


Fig. 5. Intensity vs. the Raman shift.

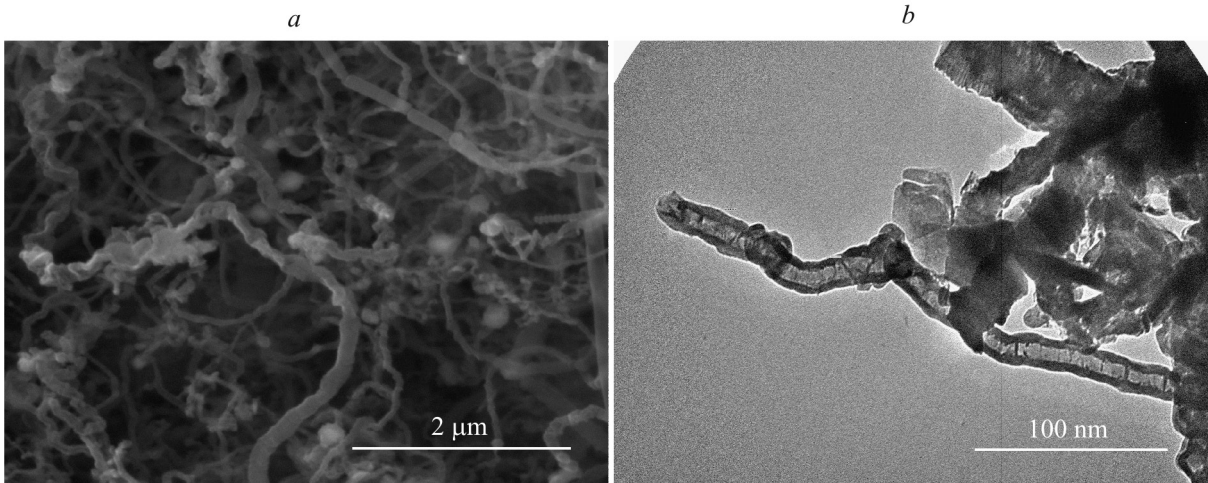


Fig. 6. Images of MWCNTs obtained by SEM (a) and TEM (b).

X-ray diffraction (XRD) enables one to analyze products by the wavelength and element strength, so that the elements in the product can be identified. Figure 7 is the XRD pattern of crude CNTs products. It can be seen from this figure that the values of d for the diffraction peaks are identical to a pyrolytic graphite. Thus, if there are nanotubes in the products, they must be CNTs. The sample contains a significant amount of nickel and silica.

Figure 8 shows the TG curve of the synthesized MWCNTs. It can be seen from this curve that in the range 650–700°C all carbon atoms were burnt. The sample obtained by CVD contains about 40 wt.% MWCNTs and amorphous carbon.

The electrochemical performance of the S/MWCNT/PAN composite which was synthesized by using MWCNTs obtained by CVD as a cathode material in Li/S batteries was further investigated by galvanostatic discharge/charge tests, and the results are shown in Fig. 9. The figure gives the nondimensional voltage \bar{U} where the voltage is related to the standard electrode potential of Li^+/Li equal to 3.05 V. There the first plateau at about 2.4 is related to the formation of higher-order lithium polysulfides (Li_2S_n , $n \geq 4$). which are soluble in a liquid electrolyte. The next prolonged plateau around the value equal to two in the discharge profiles reflects the subsequent electrochemical transition of the polysulfides to lithium sulfide $\text{Li}_2\text{S}_2/\text{Li}_2\text{S}$.

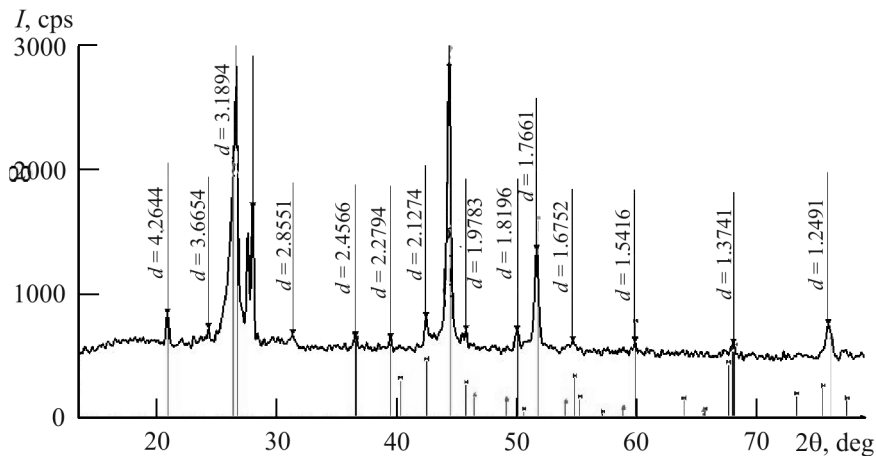
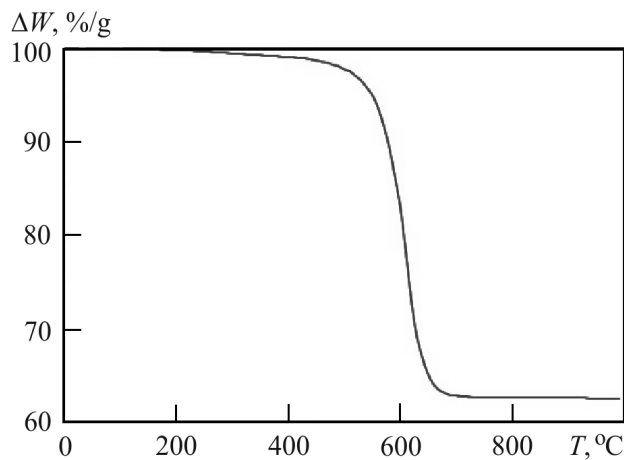
Fig. 7. X-ray diffraction pattern of MWCNTs. The values of d are given in Å.

Fig. 8. TG curve of MWCNTs.

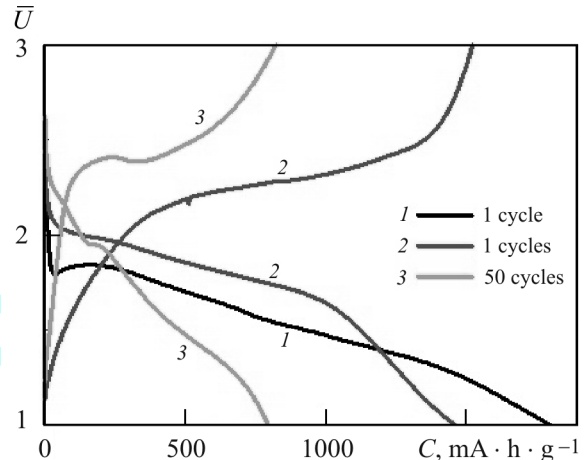


Fig. 9. Discharge/charge profiles of lithium cells with S/MWCNT/PAN composite at the C-rate 0.2 C.

As we can see in Fig. 9, the first plateau is short, and the system discharge capacity depends mainly on the second one. Starting from the following cycle, this composite exhibited the typical Li/S potential profile features associated with a reversible reaction of Li and S. The S/MWCNT/PAN composite delivers a high discharge capacity of about $1500 \text{ mA} \cdot \text{h} \cdot \text{g}^{-1}$. After fifty cycles the discharge capacity is decreased to $800 \text{ mA} \cdot \text{h} \cdot \text{g}^{-1}$.

Conclusions. The CVD method was used for synthesizing multiwalled carbon nanotubes on a shungite substrate. From the SEM and TEM images, as well as from the Raman shifts, it was confirmed that they were synthesized successfully and had an intertwined structure. The simple method based on the use of sulfur particles and the above MWCNTs has been developed for fabricating a homogeneous S/MWCNT/PAN composite. This synthesized composite has been tested as a cathode in rechargeable Li/S batteries. The S/MWCNT/PAN composite was shown to exhibit excellent performance with a high initial capacity of up to $1500 \text{ mA} \cdot \text{h} \cdot \text{g}^{-1}$ and a stabilized capacity of $800 \text{ mA} \cdot \text{h} \cdot \text{g}^{-1}$ after 50 cycles at a battery C-rate of 0.2 C. This could be attributed to a uniform dispersion of sulfur with MWCNTs through the use of a simple heat treatment method and the resulting reduction in the charge transfer impedance.

NOTATION

C , discharge capacity; c , concentration; d , lattice parameter; E , energy; I , intensity; T , temperature; U , voltage, W , weight.

REFERENCES

1. **H. B. Ray, A. Z. Anvar, and A. H. Walt**, Carbon nanotubes — The route toward application, *Science*, **297**, No. 582, 787–792 (2002).
2. **X. D. Yang**, *Fabrication and Properties of Uniformly Dispersed Carbon Nanotube Reinforced Al Composites*, Tianjin University, Tianjin (2012).
3. **Y. Zhang, Y. Zhao, T. N. Doan, A. Konarov, D. Gosselink, H. G. Soboleski, and P. Chen**, A novel sulfur/polypyrrole/multi-walled carbon nanotube nanocomposite cathode with core — Shell tubular structure for lithium rechargeable batteries, *Solid State Ionics*, **238**, 30–35 (2013).
4. **Y. Zhang, Y. Zhao, A. Yermukhambetova, Zh. Bakenov, and P. Chen**, Ternary sulfur/polyacrylonitrile/Mg_{0.6}Ni_{0.4}O composite cathodes for high performance lithium/sulfur batteries, *J. Mater. Chem.*, **A1**, 295–301 (2013).
5. **J. Wang, J. Yang, C. Wan, K. Du, J. Xie, and N. Xu**, Sulfur composite cathode materials for rechargeable lithium batteries, *Adv. Funct. Mater.*, **13**, 487–492 (2003).
6. **M. Lin, L. Zh. Houlong, W. Shuya, E. H. Kenville, S. K. Mun, C. Gil, G. H. Richard, and A. A. Lynden**, Enhanced Li–S batteries using amine-functionalized carbon nanotubes in the cathode, *ACS Nano*, **1**, No. 10, 1050–1059 (2016).
7. **U. Sh. Musina and V. V. Samonin**, Carbon-mineral composition of Koksu shungite deposit of Kazakhstan [in Russian], *Izv. St. Petersburg. Gos. Technol. Inst.*, **49**, No. 23, 79–82 (2014).
8. **X.-G. Sun, X. Wang, R. T. Mayes, and S. Dai**, Lithium–sulfur batteries based on nitrogen-doped carbon and an ionic-liquid electrolyte, *ChemSusChem*, **5**, 2079–2085 (2012).